Bol. Soc. Paran. Mat.
©SPM – E-ISSN-2175-1188
SPM: www.spm.uem.br/bspm

(3s.) **v. 2026 (44)** : 1–13.
ISSN-0037-8712
doi:10.5269/bspm.79711

Stochastic Physics-Informed Neural Networks for Solving Drug Transport Equations with Uncertain Inputs

Saadeddine Essarrout, Said Raghay and Zouhir Mahani

ABSTRACT: Accurate modeling of drug transport in biological tissues is essential for optimizing therapeutic strategies. However, traditional numerical methods such as finite differences or finite elements become computationally expensive and inefficient when accounting for uncertainties in physiological parameters, including diffusion coefficients, reaction rates, and tissue heterogeneity. In this work, we employ Physics-Informed Neural Networks (sPINN) as a direct solver for drug transport equations with random coefficients, thereby replacing conventional discretization-based approaches. The governing partial differential equations are embedded into the neural network loss function, which allows the model to enforce physical laws throughout the training process. Once trained, the sPINN is combined with Monte Carlo sampling to estimate statistical quantities of interest, such as means, variances, and confidence intervals, under different realizations of uncertain parameters. Numerical results show that the proposed method achieves accuracy comparable to reference solutions while significantly reducing computational cost. This hybrid framework, combining sPINN with Monte Carlo estimation, offers a robust and data-efficient approach for modeling drug distribution in complex biological environments under uncertainty.

Keywords: sPINN, Monte Carlo method, drug transport equations, uncertain inputs.

Contents

1. Introduction

Pharmacokinetic compartmental (PKC) models, particularly three-compartment models, form the foundation for modeling drug transport in the body and are widely used to predict the distribution, metabolism, and elimination of therapeutic substances. These models are typically represented by systems of ordinary or partial differential equations, often coupled with uncertain parameters such as inter-compartmental transfer rates and elimination rates (see Figure 1), and for further information, see [11, 12,4,?]. The presence of these uncertainties necessitates their explicit consideration. To address this, the deterministic problem is transformed into a stochastic problem by modeling the uncertain parameters as random fields. Since analytical solutions for such problems are challenging, classical numerical methods, such as finite difference schemes or finite element methods combined with Monte Carlo simulations [1,3,2,7], while effective, can become computationally expensive and sensitive to uncertainty propagation.

In the context of pharmacokinetics, the application of Physics-Informed Neural Networks (sPINN) [10] to multi-compartment models with uncertain parameters remains largely unexplored. The main challenges include managing the stochastic uncertainty of the parameters, accurately capturing the transient dynamics, and ensuring network convergence. Motivated by these issues, this study investigates the

2020 *Mathematics Subject Classification:* Primary 65M75, 65C05; Secondary 35Q92, 92C50.
Submitted October 23, 2025. Published March 22, 2026

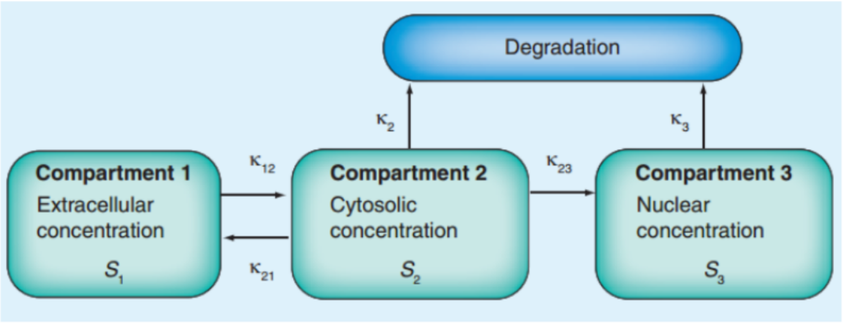

Figure 1: Three-compartment pharmacokinetic model with inter-compartmental transfer and elimination rates.

effectiveness of sPINN for solving a three-compartment drug transport model with uncertain parameters, comparing different strategies to improve convergence and accuracy, and evaluating performance against classical numerical methods.

This study aims to address the following questions:

1. Can sPINN provide a reliable framework for uncertainty quantification in differential equations arising from pharmacokinetics?
2. What improvements to the basic sPINN model are necessary to accurately and robustly solve the three-compartment system with uncertain parameters?
3. How do sPINN compare with traditional numerical methods in terms of accuracy and computational efficiency?

The paper is structured as follows. Section 2 introduces the mathematical formulation of the problem and the main notations used throughout the study. In Section 3, we describe the sPINN algorithm applied to the three-compartment drug transport model with uncertain parameters. Section 4 details the loss functions employed for training the sPINN. In Section 5, Monte Carlo estimations of statistical quantities are presented. Section 6 provides numerical experiments to validate the proposed approach. Finally, Section 7 concludes the paper and discusses potential directions for future work.

2. Problem Formulation

Deterministic Model of Drug Transport:

We consider a compartmental pharmacokinetic model describing the transport of a drug (e.g., cisplatin) across three biological compartments:

- $\mathbf{S}_1(x,t)$: extracellular drug concentration,
- $\mathbf{S}_2(x,t)$: cytosolic concentration,
- $\mathbf{S}_3(x,t)$: nuclear (DNA-bound) concentration.

Let $D \subset \mathbb{R}^2$ denote the spatial domain and $t \in [0,T]$ the time interval of interest. The governing system of partial differential equations (PDEs) is:

$$\begin{cases} \frac{\partial \mathbf{S}_1}{\partial t} = D_s \Delta \mathbf{S}_1 - k'_{12}\mathbf{S}_1 + \frac{k'_{21}}{V_c}\mathbf{S}_2, \\ \frac{\partial \mathbf{S}_2}{\partial t} = k_{12}V_c\mathbf{S}_1 - (k_{21}+k_2+k_{23})\,\mathbf{S}_2, \\ \frac{\partial \mathbf{S}_3}{\partial t} = k_{23}\mathbf{S}_2 - k_3\mathbf{S}_3, \end{cases} \tag{2.1}$$

subject to homogeneous Dirichlet boundary conditions:

$$\mathbf{S}_i(x,t) = 0 \quad \text{on} \quad \partial D \quad \text{for } i = 1,2,3. \tag{2.2}$$

and prescribed initial conditions:

$$\mathbf{S}_i(x,0) = \mathbf{S}_0 i(x) \quad \text{in} \quad D \quad \text{for } i = 1,2,3. \tag{2.3}$$

Here:

- D_s: diffusivity of the drug in tissue,
- V_c: local cell volume,
- k_{ij}: drug transfer rates between compartments
- k_i: elimination or repair rates,
- $k'_{ij} = k_{ij}/F$, where F is the extracellular volume fraction.

Incorporation of Uncertainty

In realistic biological systems, parameters such as diffusivity, volume fractions, and transfer rates are spatially heterogeneous and subject to experimental uncertainty. To account for this, we model the coefficients D_s, V_c, k_{ij}, k_i as random fields defined over a complete probability space $(\Omega, \mathfrak{F}, \mathbb{P})$. Consequently, the concentrations $\mathbf{S}_i = \mathbf{S}_i(x,t;\omega)$ also become stochastic processes.

Let $\xi = (\xi^1, \ldots, \xi^N)$ denote a set of independent random variables obtained through a finite-dimensional stochastic representation of the random fields, such as the Karhunen-Loève (KL) expansion [8]. Then, each parameter can be written as:

$$k(\omega, x) = \bar{k}(x) + \sum_{n=1}^{N} \sqrt{\lambda_n}\phi_n(x)\xi_n(\omega) \tag{2.4}$$

where $\bar{k}(x)$ is the mean, $\lambda_n, \phi_n(x)$, are eigenpairs of the covariance kernel, and $\xi_n \sim \mathcal{U}[-1,1]$ (or standard normal) are independent random variables.

The stochastic PDE system now becomes:

$$\begin{cases} \frac{\partial \mathbf{S}_1}{\partial t}(x,t;\xi) = D_s(x,\xi)\Delta\mathbf{S}_1(x,t;\xi) - k'_{12}(x,\xi)\mathbf{S}_1(x,t;\xi) + \frac{k'_{21}(x,\xi)}{V_c(x,\xi)}\mathbf{S}_2(x,t;\xi) \\ \frac{\partial \mathbf{S}_2}{\partial t}(x,t;\xi) = k_{12}(x,\xi)V_c(x,\xi)\mathbf{S}_1(x,t;\xi) - (k_{21}+k_2+k_{23})(x,\xi)\mathbf{S}_2(x,t;\xi) \\ \frac{\partial \mathbf{S}_3}{\partial t}(x,t;\xi) = k_{23}(x,\xi)\mathbf{S}_2(x,t;\xi) - k_3(x,\xi)\mathbf{S}_3(x,t;\xi) \end{cases} \tag{2.5}$$

with stochastic initial and boundary conditions:

$$\mathbf{S}_i(x,0;\xi) = \mathbf{S}_0 i(x;\xi), \qquad \mathbf{S}_i(x,t;\xi) = 0 \quad \text{on } \partial D \quad \text{for } i = 1,2,3. \tag{2.6}$$

3. Physics-Informed Neural Network Framework

Physics-Informed Neural Networks (sPINN) constitute a class of neural networks specifically designed to approximate the solutions of partial differential equations (PDEs) by directly embedding the governing equations, along with boundary and initial conditions, into the training process. Unlike traditional purely data-driven neural networks, sPINN leverage prior knowledge of the underlying physics. This is achieved by constructing a composite loss function that penalizes violations of the PDE residuals as well as deviations from boundary and initial constraints. Such a framework is particularly advantageous for solving both forward and inverse problems, especially in scenarios where the system exhibits uncertainty.

Application to Stochastic Drug Transport

In the context of stochastic drug transport modeling, the objective is to learn a functional mapping of the form:

$$(x, y, t, \xi^1, \ldots, \xi^N) \longmapsto (\mathbf{S}_1, \mathbf{S}_2, \mathbf{S}_3)\,, \tag{3.1}$$

where (x, y) denote spatial coordinates, t is the time variable, and $\xi = (\xi^1, \ldots, \xi^N)$ represents the stochastic parameters capturing uncertainties in model coefficients or initial/boundary conditions. The outputs $\mathbf{S}_i(x, y, t; \xi)$ correspond to the drug concentrations in the three compartments and are modeled as the outputs of a neural network. This formulation allows the sPINN to approximate the solution of the stochastic PDE system introduced in Section 2.

Two main strategies can be adopted to handle the stochasticity:

(A) External Monte Carlo (one network per realization). Alternatively, one can sample M realizations $\{\xi^{(m)}\}_{m=1}^{M}$ and train a separate deterministic sPINN for each realization. Although conceptually straightforward, this method is computationally intensive, as it requires training M independent networks. Efficiency can be improved using warm-starting, where the weights of one network are initialized from the previous realization's trained network.

(B) Stochastic PINN (sPINN) with Monte Carlo in the loss. In this approach, a single neural network

$$\mathcal{N}_\theta : (x, y, t, \xi) \mapsto (\hat{S}_1, \hat{S}_2, \hat{S}_3)$$

is trained to directly take the stochastic variables ξ as inputs. This network learns a simultaneous approximation of the solution across all realizations. The training loss is computed using a Monte Carlo approximation of the expected physics-informed loss, effectively integrating the stochastic dimension into the optimization process. This approach is highly efficient when estimating statistical quantities of interest such as mean, variance, or higher-order moments.

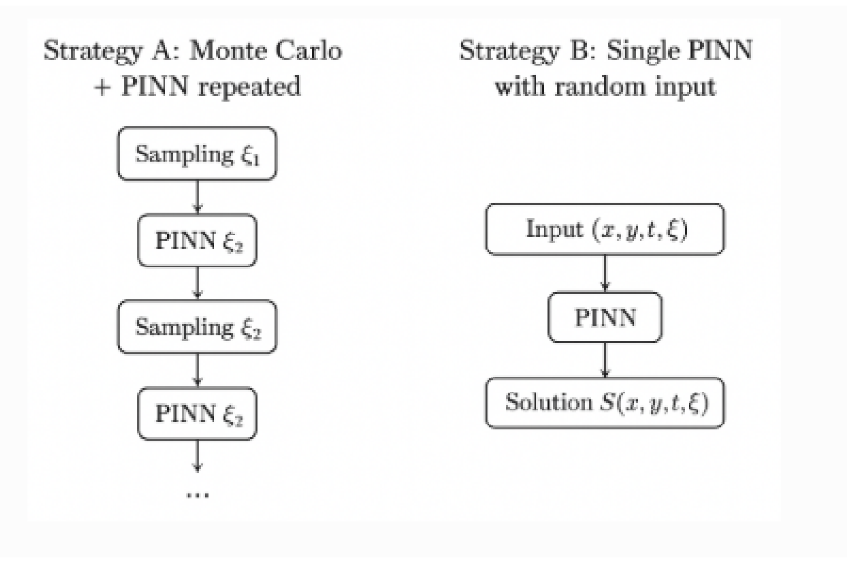

Figure 2: Illustration of Alternative Strategies for Solving with sPINN.

In this study, we adopt strategy (B), where the stochastic parameters ξ are included as network inputs and the physics-informed loss is approximated by Monte Carlo sampling. This allows a single sPINN to capture the solution across random realizations, and once trained, the same framework can be combined with external Monte Carlo sampling to estimate statistical quantities such as mean and variance with high efficiency.

Network Architecture and Initialization

The neural network weights are initialized using the Randomized Weight and Bias Fourier (RWF) technique proposed by Wang et al. [14], which improves convergence and training stability. The network architecture is defined as:

$$h^{(0)} = \sigma\Big(W^{(0)}\Phi(P(x)) + b^{(0)}\Big), \qquad \text{(input to first hidden layer)} \tag{3.2}$$

$$h^{(l)} = \sigma\Big(W^{(l)}h^{(l-1)} + b^{(l)}\Big), \qquad l = 1, 2, \dots, L \quad \text{(hidden layers)} \tag{3.3}$$

$$u = W^{(L+1)}h^{(L)} + b^{(L+1)}, \qquad \text{(output layer)} \tag{3.4}$$

where σ is the nonlinear activation function; in this work, the hyperbolic tangent function tanh is employed. The network receives spatial coordinates, time, and stochastic parameters as inputs, propagates them through L hidden layers, and outputs the approximated concentrations in the three compartments.

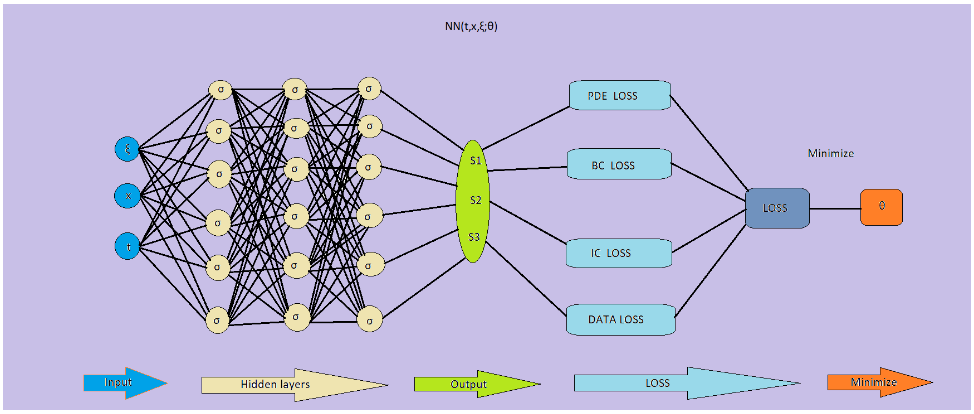

Figure 3: Schematic of the sPINN architecture applied to the 2-D stochastic pharmacokinetic equations.

4. Loss Function: sPINN with Monte Carlo Sampling

To incorporate parametric uncertainty during training, we use Monte Carlo sampling to approximate the expectation integrals in the loss function. At each training iteration, a mini-batch of random parameters

$$\xi^{(b)}, \quad b = 1, \dots, B_\xi,$$

is drawn, and for each realization, collocation points (x_j, y_j, t_j) are sampled in the physical domain. The empirical loss functional is then computed as

$$\begin{aligned}\mathcal{L}(\theta) = {} & \lambda_{\text{PDE}} \frac{1}{B_\xi} \sum_{b=1}^{B_\xi} \frac{1}{N_f} \sum_{j=1}^{N_f} \sum_{i=1}^{3} \mathcal{R}_i^2(x_j, y_j, t_j; \xi^{(b)}) \\ & + \lambda_{\text{IC}} \frac{1}{B_\xi} \sum_{b=1}^{B_\xi} \frac{1}{N_0} \sum_{k=1}^{N_0} \sum_{i=1}^{3} \big|\hat{S}_i(x_k, y_k, 0; \xi^{(b)}) - S_{0i}(x_k, y_k; \xi^{(b)})\big|^2 \\ & + \lambda_{\text{BC}} \frac{1}{B_\xi} \sum_{b=1}^{B_\xi} \frac{1}{N_b} \sum_{r=1}^{N_b} \sum_{i=1}^{3} \big|\hat{S}_i(x_r, y_r, t_r; \xi^{(b)})\big|^2,\end{aligned} \tag{4.1}$$

where $\lambda_{\text{PDE}}, \lambda_{\text{IC}}, \lambda_{\text{BC}}$ are penalty parameters. The residuals $\mathcal{R}_i$ correspond to the stochastic three-compartment PDE system and are given by

$$\mathcal{R}_1 = \frac{\partial \hat{S}_1}{\partial t} - D_s(x,\xi)\,\Delta \hat{S}_1 + k'_{12}(x,\xi)\hat{S}_1 - \frac{k'_{21}(x,\xi)}{V_c(x,\xi)}\hat{S}_2, \tag{4.2}$$

$$\mathcal{R}_2 = \frac{\partial \hat{S}_2}{\partial t} - k_{12}(x,\xi)V_c(x,\xi)\hat{S}_1 + \big(k_{21} + k_2 + k_{23}\big)(x,\xi)\,\hat{S}_2, \tag{4.3}$$

$$\mathcal{R}_3 = \frac{\partial \hat{S}_3}{\partial t} - k_{23}(x,\xi)\hat{S}_2 + k_3(x,\xi)\hat{S}_3. \tag{4.4}$$

In practice, mini-batching is performed both in the random space (over the realizations B_ξ) and in the physical space (over collocation, initial, and boundary points N_f, N_0, N_b). The optimization procedure first employs the Adam optimizer for robustness, followed by L-BFGS for fine convergence. All gradients are computed using automatic differentiation.

Remark: Monte Carlo sampling is used *during training* to approximate the expectation integrals in the loss function. After training, a separate Monte Carlo procedure is applied to the trained sPINN to estimate statistical quantities such as mean, variance, or other moments. This distinction ensures that Monte Carlo serves both as a tool for stochastic approximation in the loss and for post-training uncertainty quantification.

5. Monte Carlo Estimation of Statistical Quantities

Once the surrogate model $\mathcal{N}_\theta$ has been trained, statistical quantities of interest (QoIs) are estimated through a standard Monte Carlo (MC) procedure. Specifically, we evaluate $\mathcal{N}_\theta$ at a set of independent and identically distributed (i.i.d.) realizations of the random parameters

$$\xi^{(m)}, \quad m = 1, \dots, M.$$

For each solution component S_i, the empirical mean field is computed as

$$\widehat{\mathbb{E}}[S_i](x,y,t) = \frac{1}{M}\sum_{m=1}^{M} \hat{S}_i(x,y,t;\xi^{(m)}),$$

while the empirical variance reads

$$\widehat{\mathrm{Var}}[S_i](x,y,t) = \frac{1}{M-1}\sum_{m=1}^{M}\Big(\hat{S}_i(x,y,t;\xi^{(m)}) - \widehat{\mathbb{E}}[S_i](x,y,t)\Big)^2.$$

In addition to the solution fields, one often considers generic quantities of interest $Q(S)$, such as the total mass of drug or the dose at the nucleus. For such a QoI, the Monte Carlo estimator of the expectation is

$$\widehat{\mathbb{E}}[Q] = \frac{1}{M}\sum_{m=1}^{M} Q\big(\hat{S}(\cdot;\xi^{(m)})\big).$$

To assess statistical reliability, we compute confidence intervals for these estimators. Assuming approximate normality, the 95% confidence interval of Q is given by

$$CI_{95\%} \;\approx\; \widehat{\mathbb{E}}[Q] \;\pm\; 1.96\,\frac{\hat{\sigma}_Q}{\sqrt{M}},$$

where $\hat{\sigma}_Q$ is the empirical standard deviation of Q:

$$\hat{\sigma}_Q^2 = \frac{1}{M-1}\sum_{m=1}^{M}\Big(Q(\hat{S}(\cdot;\xi^{(m)})) - \widehat{\mathbb{E}}[Q]\Big)^2.$$

6. Results and Discussion

To demonstrate the effectiveness of the proposed method, we perform two numerical tests in this section with the following deterministic initial condition:

$$S_1^0(x,y) = 0.05\,\mathrm{kg/m}^3, \quad S_2^0(x,y) = 0.05\,\mathrm{kg/m}^3, \quad S_3^0(x,y) = 0.05\,\mathrm{kg/m}^3.$$

The parameters k_{12}, k_{21}, k'_{12}, k'_{21}, k_2, k_3, V_c, and D_s are chosen as follows:

$$\begin{aligned}
V_c(x,y,\xi) &= \left|520\cdot 10^{-6} + 10^{-4}\cdot \sin\big((\xi_1+\xi_2+\xi_3)x - (\xi_4+\xi_5+\xi_6)y\big)\right|,\\
k_{12}(x,y,\xi) &= \left|1.48 - 0.1\cdot \sin\big((\xi_1+\xi_2+\xi_3)x - (\xi_4+\xi_5+\xi_6)y\big)\right|,\\
k'_{12}(x,y,\xi) &= \frac{k_{12}(x,y,\xi)}{0.48},\\
k_{21}(x,y,\xi) &= \left|0.071 + 0.1\cdot \cos\big((\xi_1+\xi_2+\xi_3)x - (\xi_4+\xi_5+\xi_6)y\big)\right|,\\
k'_{21}(x,y,\xi) &= \frac{k_{21}(x,y,\xi)}{0.48},\\
k_{2}(x,y,\xi) &= \left|1.55 + 0.5\cdot \sin\big((\xi_1+\xi_2+\xi_3)x + 2(\xi_4+\xi_5+\xi_6)y\big)\right|,\\
k_{23}(x,y,\xi) &= \left|11.8 + 0.1\cdot \sin\big((\xi_1+\xi_2+\xi_3)x - 2(\xi_4+\xi_5+\xi_6)y\big)\right|,\\
k_{3}(x,y,\xi) &= \left|0.95 + 0.2\cdot \sin\big((\xi_1+\xi_2+\xi_3)x - (\xi_4+\xi_5+\xi_6)y\big)\right|,\\
D_s(x,y,\xi) &= \left|0.003 + 10^{-2}\cdot \sin\big((\xi_1+\xi_2+\xi_3)x - (\xi_4+\xi_5+\xi_6)y\big)\right|,
\end{aligned}$$

where $(x,y)\in D = [0,1]\times[0,1]$ and ξ_k $(0\le k\le 6)$ is an independent random variable uniformly distributed over $[0,1]$.

To study the training dynamics of the PINN for stochastic drug transport in two dimensions, we consider the spatial domain $(x,y)\in D\subset\mathbb{R}^2$ and a temporal interval $t\in[0,T]$. The concentrations in the three compartments are denoted by $S_1(x,y,t;\xi)$, $S_2(x,y,t;\xi)$, and $S_3(x,y,t;\xi)$, depending on the random variables $\xi = (\xi^1,\dots,\xi^N)$ representing uncertainties in the pharmacokinetic parameters.

Boundary Conditions (Homogeneous Cauchy). All concentrations are zero on the boundaries of the spatial domain:

$$S_k(x,y,t;\xi) = 0, \quad \forall (x,y)\in\partial D, \quad k = 1,2,3.$$

The loss associated with the boundary conditions is then:

$$\mathcal{L}_{\mathrm{BC}} = \frac{1}{N_t N_{\mathrm{b}}}\sum_{i=1}^{N_t}\sum_{(x_b,y_b)\in\partial D}\sum_{k=1}^{3}\big(S_k(x_b,y_b,t_i;\xi)\big)^2,$$

where N_{b} is the number of collocation points on the boundaries.

Initial Conditions. At $t=0$, the concentrations are non-zero in the spatial domain, corresponding to the initial state of the drug in each compartment:

$$\mathcal{L}_{\mathrm{IC}} = \frac{1}{N_x N_y}\sum_{i=1}^{N_x}\sum_{j=1}^{N_y}\sum_{k=1}^{3}\big(S_k(x_i,y_j,t=0;\xi) - S_k^{\mathrm{init}}(x_i,y_j)\big)^2,$$

where $S_k^{\mathrm{init}}(x,y)$ represents the known or measured initial distribution of the drug in compartment k, and $N_x\times N_y$ is the number of collocation points in the domain D.

Residual Loss. The residual loss is computed from the stochastic transport equations for each compartment:

$$\mathcal{L}_{\mathrm{res}} = \frac{1}{N_t N_x N_y}\sum_{i=1}^{N_x}\sum_{j=1}^{N_y}\sum_{\ell=0}^{N_t}\sum_{k=1}^{3}\left[\left(\frac{\partial S_k}{\partial t}(x_i,y_j,t_\ell;\xi) - f_k(S_1,S_2,S_3;\xi)\right)^2\right],$$

where f_k represents the transfers and degradation specific to compartment k.

Total Loss. The total loss used for PINN training is:

$$\mathcal{L}_{\text{total}} = w_{\text{IC}}\mathcal{L}_{\text{IC}} + w_{\text{BC}}\mathcal{L}_{\text{BC}} + w_{\text{res}}\mathcal{L}_{\text{res}}.$$

This 2D formulation with homogeneous Cauchy boundary conditions and non-zero initial conditions allows the sPINN to accurately capture the spatial and temporal distribution of concentrations in the three compartments while incorporating uncertainties in the model parameters.

The penalization parameters in the total loss are chosen as follows:

$$w_{\text{IC}} = 10, \quad w_{\text{BC}} = 10, \quad w_{\text{res}} = 20,$$

reflecting the relative importance of satisfying the transport equations compared to the initial and boundary conditions. These values were determined empirically to ensure stable convergence and good model accuracy.

Test1:

First, it is essential to analyze the influence of the number of realizations M on the statistical accuracy of the obtained results. Indeed, both the mean of the solution and the confidence interval directly depend on the value of M. As illustrated in Figure 4, when the number of realizations is small, the estimates exhibit significant variability and the confidence intervals remain relatively wide, reflecting a high level of uncertainty in the results. As M increases, the law of large numbers comes into play: the mean progressively stabilizes toward a value representative of the true expectation, and the confidence interval narrows significantly. Therefore, choosing a sufficiently large number of realizations reduces uncertainty, enhances the robustness of numerical estimates, and ensures the reliability of statistical conclusions. This step is thus fundamental to guarantee that the results are not driven by artifacts due to an insufficient sample size, but rather reflect the general trend of the studied phenomenon.

Next, to check the convergence of the proposed method, we solve the following system

$$\begin{cases} \dfrac{\partial S_1}{\partial t} = D_s \Delta S_1 - k'_{12} S_1 + k'_{21} V_c S_2 + h_1, \\ \dfrac{\partial S_2}{\partial t} = k_{12} V_c S_1 - k_{21} S_2 - k_2 S_2 - k_{23} S_2 + h_2, \\ \dfrac{\partial S_3}{\partial t} = k_{23} S_2 - k_3 S_3 + h_3, \end{cases}$$

where the functions h_1, h_2, and h_3 are the added source terms used to construct exact solutions. The exact solutions are given by

$$S_1(x, y, t, \xi) = xy(1-x)(1-y)\, \exp(D_s + (k'_{12} + k'_{21})(x, y, \xi)) \exp(-V_c(x, y, \xi)\, t)\,,$$

$$S_2(x, y, t, \xi) = xy(1-x)(1-y)\, \exp((k_{12}V_c - k_{21} - k_2)(x, y, \xi)) \exp(-k_{23}(x, y, \xi)\, t)\,,$$

$$S_3(x, y, t, \xi) = xy(1-x)(1-y)\, \exp(k_{23}(x, y, \xi) + x + y) \exp(-k_3(x, y, \xi)\, t)\,.$$

The error for the mean and the variance of the solution is given and compared betwin the sPINN and FDM [5] for different values of the number of realizations M where the values of the parameter of the difference scheme $\Delta x = \Delta y = 0.001$ are given in the tables.

The table clearly shows that increasing the number of realizations improves the accuracy of the statistical estimates (mean and variance), and that the sPINN method is capable of providing reliable approximations comparable to those of the classical finite difference method, even for complex stochastic systems, which confirms the reliability of our approach.

Test2:

In the second test, the analysis begins with the resolution of the deterministic problem, where the model is evaluated using the fixed set of parameters presented in Table 2. This initial step allows for a comparison of the curves obtained for case 1 and case 2, thereby highlighting the differences arising

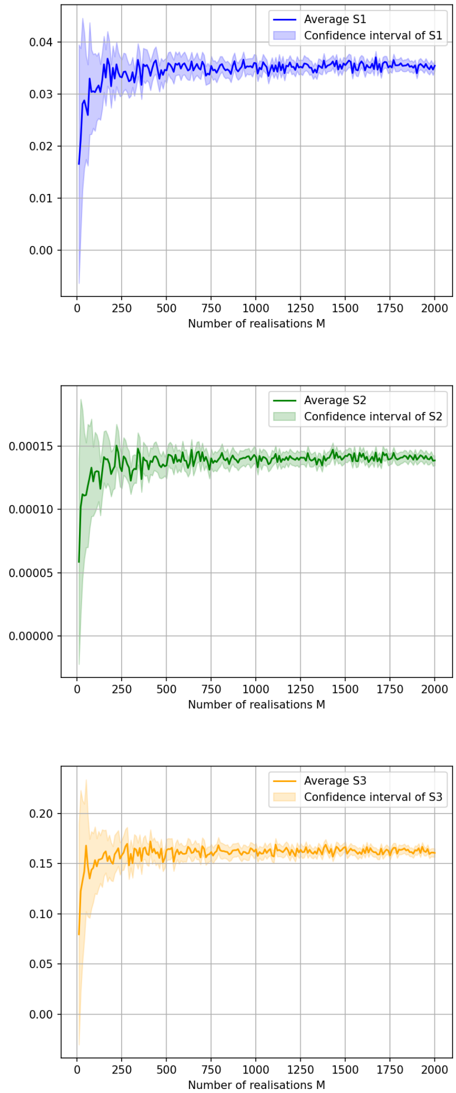

Figure 4: The confidence interval for $\bar{\mu}$ at the 95% level.

Table 1: Error for the mean and the variance of the solution components S_1, S_2, S_3 obtained by sPINN and FDM for different values of the number of realizations M with $\Delta x = \Delta y = 0.001$.

M	Component	Mean error		Variance error	
		sPINN	FDM	sPINN	FDM
500	S_1	1.2×10^{-1}	1.0×10^{-1}	2.1×10^{-1}	1.9×10^{-1}
	S_2	1.5×10^{-1}	1.1×10^{-1}	2.4×10^{-1}	2.0×10^{-1}
	S_3	1.0×10^{-1}	2.2×10^{-1}	1.9×10^{-1}	1.6×10^{-1}
1000	S_1	6.5×10^{-2}	5.0×10^{-2}	1.2×10^{-2}	1.0×10^{-2}
	S_2	7.0×10^{-2}	5.5×10^{-2}	1.3×10^{-2}	1.1×10^{-2}
	S_3	5.8×10^{-2}	4.2×10^{-2}	1.1×10^{-2}	9.0×10^{-3}
10000	S_1	3.2×10^{-4}	2.5×10^{-4}	7.5×10^{-4}	6.5×10^{-4}
	S_2	3.5×10^{-4}	2.8×10^{-4}	7.8×10^{-4}	6.8×10^{-4}
	S_3	2.9×10^{-4}	2.3×10^{-4}	6.9×10^{-4}	5.9×10^{-4}

from the choice of parameters and emphasizing the potential presence of uncertainties. In a second stage, the stochastic problem is addressed through the proposed stochastic Physics-Informed Neural Network (sPINN) approach, which explicitly accounts for uncertainties in the model parameters. This framework enables the neural network to capture not only the average behavior of the system but also the variability induced by random fluctuations in the parameters. To rigorously assess both the accuracy and the efficiency of the sPINN method, the solutions obtained are systematically compared with those provided by the classical finite difference method, which serves as a benchmark in the referenced study. The results of this comparison, illustrated in Figure 5, highlight the capability of the sPINN to provide reliable approximations while effectively handling the stochastic nature of the problem.

In particular, the solution we used for comparison is exactly the mean approximated solution by different random parameters than the first test and which reads

Table 2: Values of parameters for Cisplatin (from Sinek et al., Tröger et al., Lavasseur et al. and associated references).

Parameter	**Description**	**Case 1 value**	**Reference**	**Case 2 value**	**Reference**
V_C	Cell volume (fL cell^{-1})	520	Sinek et al. [12]	520	Sinek et al. [12]
F	Interstitial Fraction	0.48	–	0.48	–
D_s	Drug diffusivity (μm^2 min^{-1})	3.0×10^4	–	3.0×10^4	–
k_2	Inactivation rate (min^{-1})	1.7	–	1.7	–
k_{12}	Drug uptake (min^{-1})	0.043	Tröger et al. [13]	0.00545	Lavasseur et al. [9]
k_{21}	Drug efflux (min^{-1})	0.00197	–	0.0004	–
k_{23}	Drug-DNA binding (min^{-1})	0.00337	–	0.06242	–
k_3	Drug-DNA repair (min^{-1})	0.00785	–	0.02402	–

The values of k_{12}, k_{21}, k_{23} and k_3 can be found in [4] (Table 3, Peak-bound intracellular model), and k'_{12}, k'_{21} are obtained using the formula

$$k'_{ij} = \frac{k_{ij}}{F}, \quad i, j \in \{1, 2\}.$$

Figure 5 shows the general behavior of the variation of cisplatin concentration in the three compartments as a function of time, for two deterministic cases and for the stochastic case. The optimal parameters obtained in the two cases presented in Table 2 provide reasonably good results, but with insufficient accuracy due to the differences between case 1 and case 2, as clearly illustrated by the blue and yellow curves. To overcome this issue, we use the stochastic method, which yields the results represented by the red curve for the proposed method (sPINN) and the green curve for the finite difference method (see [5]).

As illustrated in Figure 5, the dynamic profiles of cisplatin concentration in the three compartments exhibit significant variations over time for the two specific deterministic cases described in Table 2. However, the optimally adjusted parameters in these deterministic scenarios appear implausible, as evidenced by the inaccuracies in the obtained results. To address this problem, we introduced stochasticity into the model by assigning a random nature to the parameters, thereby providing a more realistic representation of the system's behavior, as shown in Figure 5.

Our approach based on stochastic sPINN offers a more detailed and nuanced understanding of pharmacokinetic dynamics, taking into account the uncertainties and variability inherent in biological systems. The results demonstrate the relevance of our method compared to the combination of the finite difference method and Monte Carlo simulations (see [5]), with the curves showing striking similarities. This agreement highlights the robustness of our approach, ensuring model predictions that are both valid and accurate.

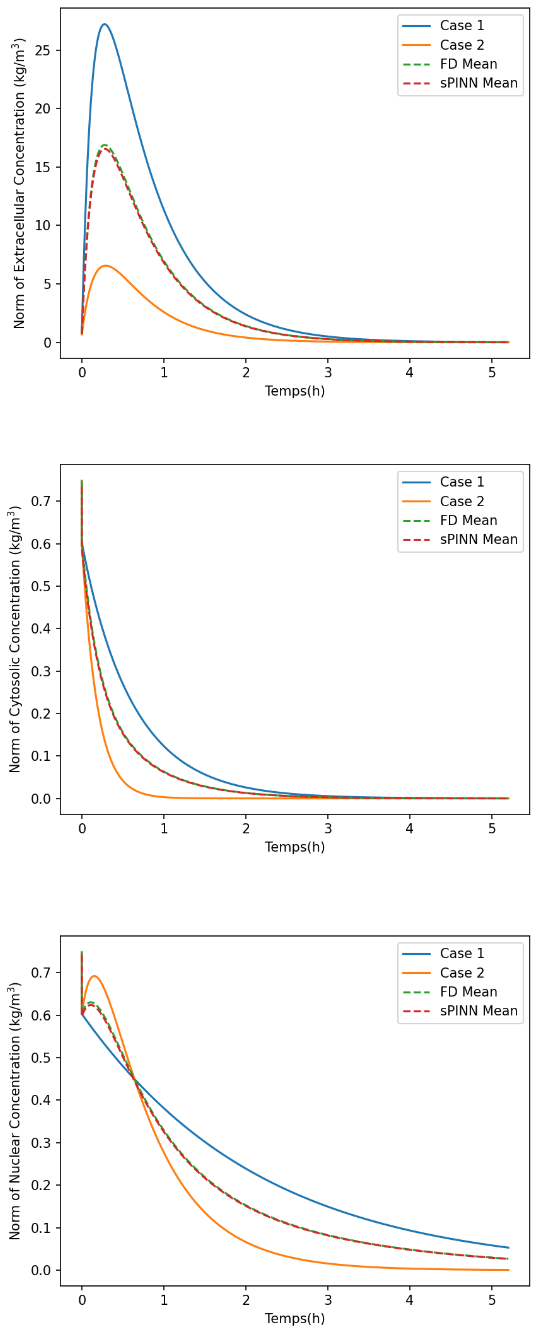

Figure 5: Deterministic and stochastic results obtained using sPINN and FD.

7. Conclusion

In this work, we have presented a stochastic Physics-Informed Neural Network (sPINN) framework for solving drug transport equations with random coefficients. By embedding the parametric uncertainty directly into the neural network, our method allows the solution to capture the effects of variability in physiological parameters without relying on repeated deterministic simulations.

The combination of PINNs with Monte Carlo sampling enables the efficient estimation of statistical quantities such as mean and variance, while maintaining high accuracy in approximating the underlying partial differential equations. Numerical experiments demonstrate that the sPINN approach can generate a large number of virtual realizations rapidly, providing detailed insights into the uncertainty propagation in drug concentrations across compartments.

Overall, this study highlights the potential of sPINNs as a powerful alternative to classical numerical methods for uncertain PDEs in pharmacokinetics, offering both computational efficiency and flexibility in handling complex stochastic models. Future work will explore extensions to more complex geometries, time-dependent uncertainties, and multi-scale pharmacological models.

References

1. A. Barth, C. Schwab, and N. Zollinger, Multi-level Monte Carlo finite element method for elliptic PDEs with stochastic coefficients, *Numerische Mathematik*, 119 (2011), 123–161.
2. A. Barth and A. Lang, Multilevel Monte Carlo method with applications to stochastic partial differential equations, *International Journal of Computer Mathematics*, 89 (18) (2012), 2479–2498.
3. K. A. Cliffe, M. B. Giles, R. Scheichl, and A. L. Teckentrup, Multilevel Monte Carlo methods and applications to elliptic PDEs with random coefficients, *Computing and Visualization in Science*, 14 (2011), 3.
4. A. W. El-Kareh and T. W. Secomb, A mathematical model for cisplatin cellular pharmacodynamics, *Neoplasia*, 5 (2) (2003), 161–169.
5. S. Essarrout, Z. Mahani, and S. Raghay, Quantifying uncertainty of a mathematical model of drug transport in tumors, *Mathematical Modeling and Computing*, 9 (3) (2022), 65–77.
6. S. Essarrout, S. Raghay, and Z. Mahani, Regularity analysis and numerical resolution of the pharmacokinetics equation for cisplatin with random coefficients and initial conditions, *Journal of Mathematical Modeling*, Research Article (2020), DOI: 10.22124/jmm.2020.16520.1433.
7. S. Essarrout, S. Raghay, and Z. Mahani, Well-posedness and convergence analysis of the multi-level Monte Carlo method for a system of PDEs with random coefficients modeling drug transport in tumors, *Advanced Mathematical Models & Applications*, 9 (3) (2024), 454–474.
8. R. Ghanem and P. D. Spanos, *Stochastic Finite Elements: A Spectral Approach*, Dover Publications, 2003.
9. L. M. Levasseur, H. K. Slocum, Y. M. Rustum, and W. R. Greco, Modeling of the time-dependency of in vitro drug cytotoxicity and resistance, *Cancer Research*, 58 (24) (1998), 5749–5761.
10. M. Raissi, P. Perdikaris, and G. E. Karniadakis, Physics-informed neural networks: A deep learning framework for solving forward and inverse problems involving nonlinear partial differential equations, *Journal of Computational Physics*, 378 (2019), 686–707.
11. S. Sandeep, J. P. Sinek, H. B. Frieboes, M. Ferrari, J. P. Fruehauf, and V. Cristini, Mathematical modeling of cancer progression and response to chemotherapy, *Expert Review of Anticancer Therapy*, 6 (10) (2006), 1361–1376.
12. J. P. Sinek, S. Sanga, X. Zheng, H. B. Frieboes, M. Ferrari, and V. Cristini, Predicting drug pharmacokinetics and effect in vascularized tumors using computer simulation, *Journal of Mathematical Biology*, 58 (2008), 485.
13. V. Troger, J. L. Fischel, P. Formento, J. Gioanni, and G. Milano, Effects of prolonged exposure to cisplatin on cytotoxicity and intracellular drug concentration, *European Journal of Cancer*, 28 (1) (1992), 82–86.
14. S. Wang, H. Wang, J. H. Seidman, and P. Perdikaris, Random weight factorization improves the training of continuous neural representations, *arXiv preprint arXiv:2210.01274*, 2022.

Saadeddine Essarrout,

Department of Science Computing,

National Schools of Applied Sciences University Ibn Zohr,

Agadir, Morocco.

E-mail address: saadeddinemocasim@gmail.com

and

Said Raghay,
Department of Mathematic,
Faculty of Science and Techniques, Cadi Ayyad University,
Marrakesh, Morocco.
E-mail address: s.raghay@uca.ac.ma

and

Zouhir Mahani,
Department of Science Computing,
National Schools of Applied Sciences University Ibn Zohr,
Agadir, Morocco.
E-mail address: zouhir.mahani@gmail.com